Original Research Article

# Structure-guided engineering of transcriptional activator XYR1 for inducer-free production of lignocellulolytic enzymes in *Trichoderma reesei*

Qinqin Zhao [a], Zezheng Yang [b], Ziyang Xiao [a], Zheng Zhang [a], Jing Xing [a], Huiqi Liang [a], Liwei Gao [c], Jian Zhao [a], Yinbo Qu [a], Guodong Liu [a,b,*]

[a] *State Key Laboratory of Microbial Technology, Shandong University, Qingdao, 266237, China*
[b] *Taishan College, Shandong University, Qingdao, 266237, China*
[c] *Tobacco Research Institute of Chinese Academy of Agricultural Sciences, Qingdao, 266101, China*

A B S T R A C T

The filamentous fungus *Trichoderma reesei* is widely used for the production of lignocellulolytic enzymes in industry. XYR1 is the major transcriptional activator of cellulases and hemicellulases in *T. reesei*. However, rational engineering of XYR1 for improved lignocellulolytic enzymes production has been limited by the lack of structure information. Here, alanine 873 was identified as a new potential target for the engineering of XYR1 based on its structure predicted by AlphaFold2. The mutation of this residue to tyrosine enabled significantly enhanced production of xylanolytic enzymes in the medium with cellulose as the carbon source. Moreover, xylanase and cellulase production increased by 56.7- and 3.3-fold, respectively, when glucose was used as the sole carbon source. Under both conditions, the improvements of lignocellulolytic enzyme production were higher than those in the previously reported V821F mutant. With the enriched hemicellulases and cellulases, the crude enzymes secreted by the A873Y mutant strain produced 51 % more glucose and 52 % more xylose from pretreated corn stover than those of the parent strain. The results provide a novel strategy for engineering the lignocellulolytic enzyme-producing capacity of *T. reesei*, and would be helpful for understanding the molecular mechanisms of XYR1 regulation.

## 1. Introduction

The production of highly-efficient and low-cost lignocellulolytic enzymes is important for bioconversion of plant cell wall resources [1]. Filamentous fungi are mainly used for the production of lignocellulolytic enzymes (e.g. cellulases and xylanases) in industry, and the expression of these enzymes are strictly controlled by a set of transcription factors [2,3]. Consequently, engineering the abundance and/or activity of transcription factors has been proved to be a useful strategy to enhance the production of lignocellulolytic enzymes in several fungal species [4, 5].

*Trichoderma reesei* is one of the most widely used industrial producers of cellulases and xylanases [6–8]. In *T. reesei*, the $Zn_2Cys_6$ transcription factor XYR1 activates the expression of a major part of cellulases and xylanase genes [9,10]. XYR1 is *de novo* synthesized in response to lignocellulolytic enzyme-inducers (e.g. sophorose) [11], and activates the transcription of its target genes via recruiting the Mediator complex

and RNA polymerase II [12]. A single point mutation A824V was identified in XYR1 in a xylanase hyper-producing *T. reesei* strain Iogen-M8, and this mutation was shown to render inducer-independent expression of both cellulases and xylanases [13]. Mutation of the corresponding alanine residue in XlnR (homolog of XYR1) to valine, isoleucine and tyrosine also resulted in significantly increased production of xylanases and cellulases in fungus *Penicillium oxalicum* [14].

Another constitutively active mutant of XYR1 homologs was first reported in *Aspergillus niger*. Specifically, the single point mutation V756F in *A. niger* XlnR led to improved induction and derepressed expression of xylanases [15]. Through the overexpression of XYR1 carrying the same amino acid substitution (V821F), *T. reesei* strains with the capacity to express cellulase with glucose as the sole carbon source were constructed [16,17]. This allows high-level production of cellulases via continuous feeding of low-cost soluble sugars (e.g. sucrose). Mutations of several other amino acid residues around V821 and A824, including T817, E825 and A826, were also reported to increase the production of

cellulases and xylanases in *T. reesei* [18]. Recently, two basic amino acids, R434 and K861, were identified as new targets for conferring constitutively active activity on XYR1 [19]. Nevertheless, the engineering of XYR1 still lacks rational strategies because of the poor knowledge on its acting mechanism.

The fast development of bioinformatics tools for accurate prediction of protein structures facilitated the understanding and rational engineering of proteins [20]. Based on the three-dimensional structures, key amino acid residues in transcription factors can be selected for rational or semi-rational mutations to tune their characteristics, such as ligand affinity [21,22]. On the other hand, CRISPR/Cas9-based genome editing has been used to generate saturated mutations at a defined genome site, which allowed rapid evaluation of the biological consequences of sequence variations [23,24]. To our knowledge, CRISPR/Cas9-based saturated mutagenesis has not been used in the engineering of *T. reesei* for improved lignocellulolytic enzyme production.

In this study, we identified alanine 873 as a potential target for engineering the activity of *T. reesei* XYR1, and performed random mutagenesis of this site to obtain a novel constitutively active mutant. The expression patten of lignocellulolytic enzymes of the mutant strain was compared with that of the parent strain, and the enzymes produced by the mutant was investigated for hydrolysis efficiency towards lignocellulosic feedstocks.

## 2. Materials and methods

### 2.1. Strains and cultivation

*T. reesei* QMP, an uracil auxotrophic strain derived from the strain QM9414 (ATCC 26921) through deleting the *pyr4* gene, was used as a parent for strain construction. *Escherichia coli* Trans5α (TransGen Biotech, Beijing, China) was used for plasmid construction.

*T. reesei* strains were cultivated on potato dextrose agar plates at 30 °C for 5 days for conidiation. For enzyme production and RNA extraction, the strains were cultivated in 50 ml of seed medium (containing, in g/L, glucose 20.0, $(NH_4)_2SO_4$ 5.0, $KH_2PO_4$ 15.0, $MgSO_4·7H_2O$ 0.6, $CaCl_2$ 0.6, peptone 2.0, $FeSO_4·7H_2O$ 0.005, $MnSO_4·H_2O$ 0.0016, $ZnSO_4·7H_2O$ 0.0014, and $CoCl·6H_2O$ 0.002) in 300 ml Erlenmeyer flasks for 24 h at 30 °C and 200 rpm on a rotary shaker. The culture was then inoculated into the medium containing indicated carbon source and (in g/L) corn steep liquor 20.0, $KH_2PO_4$ 5.0, $(NH_4)_2SO_4$ 2.0, $MgSO_4·7H_2O$ 0.6, and $CaCl_2$ 1.0, with an inoculation ratio of 10 % (v/v), and cultivated at 30 °C and 200 rpm. Uracil with a final concentration of 1 g/L was added to the medium for uracil auxotrophic strains.

### 2.2. Strain construction

The A873 codon of XYR1 in strain QMP was mutated using the previously described CRISPR/Cas9-mediated genome editing method [25]. The 5S rRNA promoter and the guide RNA backbone were fused together using overlap extension PCR, with a spacer sequence (AGCGTCTCCAAGCGTCATCA) introduced in between. The obtained guide RNA expression cassette was directly cloned to the plasmid containing the expression cassettes of *Spcas9* and *pyrG*, and autonomously replicating sequence AMA1, using the ClonExpress II One Step Cloning Kit (Vazyme, Nanjing, China). To construct the donor template, the 1.1-kb sequence upstream of A873 codon of XYR1, the 0.4-kb downstream sequence from C874 codon, and a 980-bp fragment downstream of coding region, were amplified and fused together. A mutated protospacer adjacent motif (PAM) and NNK sequence were introduced between the first two fragments. A 32-bp sequence from *A. niger* (CATTAGGTCTGACTGACAGCACGGCGCCATGC) was introduced between the middle and third fragments as a selective site for PCR validation of strains. The donor template was finally obtained by nested PCR using the primers xyr1-873m-UF and xyr1-873m-DR. The strain carrying the xyr1V821F mutation was constructed in a similar way, with

CGTGACGGCGACGAGCCACG selected as the protospacer sequence and PAM sequence mutated to CTG. The transformants obtained from protoplast-mediated transformation were purified, and their genotypes were analyzed by PCR and Sanger sequencing. All the primers used for strain construction and identification are listed in Table S1.

### 2.3. Enzyme assays and SDS-PAGE analysis

The culture broth was centrifuged at 10,000 rpm, 4 °C for 10 min to collect supernatant. The filter paper enzyme, xylanase, cellobiohydrolase, β-xylosidase, and α-L-arabinofuranosidase activities of culture supernatants were measured using Whatman No. 1 filter paper, beech wood xylan (Yuanye Bio-Technology, China), *p*-nitrophenyl-β-D-cellobioside (*p*NPC, Sigma-Aldrich), *p*-nitrophenyl-β-D-xylopyranoside (*p*NPX, Sigma-Aldrich), *p*-nitrophenyl-α-L-arabinofuranoside (*p*NPA, Sigma-Aldrich) as the substrate respectively, as described previously [26]. One unit of enzyme activity was defined as the amount of enzyme that liberates 1 μmol of glucose/xylose equivalent or *p*-nitrophenol from the substrate per minute. The concentration of extracellular proteins was measured using the Modified Bradford reagent (Sangon, Shanghai, China). For SDS-PAGE, equal volumes (24 μl) of culture supernatants were supplemented with 5 × SDS sample loading buffer (GenStar, Beijing, China), boiled for 10 min, and loaded onto a 12 % SDS polyacrylamide separating gel for electrophoresis at 120 V for 1.0–1.5 h.

### 2.4. RNA extraction and RT-qPCR

Mycelia were harvested by vacuum filtration and frozen immediately in liquid nitrogen. Total RNA extraction and cDNA synthesis were performed as previously described [27]. qPCR analysis was performed on LightCycler 480 II system (Roche) using TB Green *Premix Ex Taq* II (Tli RNaseH Plus) (TaKaRa, Japan) according to the manufacturer's instructions. The reaction procedure of qPCR included 95 °C for 30 s, and then 40 cycles of amplification (95 °C for 5 s and 60 °C for 30 s). The transcript levels were analyzed using the $2_T^{-\Delta\Delta C}$ method using *sar1* gene as a reference [28,29]. The primers used for qPCR are listed in Table S2.

### 2.5. Saccharification of lignocellulosic biomass

Corn fiber was provided by Juneng Golden Corn Co., Ltd. (Shouguang, China) and was ground as previously described [30]. Alkali pretreated corn stover was prepared by treating cut materials in NaOH solution (0.01 g per g substrate) at 150 °C for 1 h with a solid-liquid ratio of 1:10 (w/v), followed by separating the solids and washing them to neutral pH. The saccharification experiments were carried out in 100 ml Erlenmeyer flasks with a total volume of 20 ml. The system consists of lignocellulosic biomass at a concentration of 10 % (w/v, dry weight), crude enzymes with a dosage of 10 mg/g dry substrate, and citric acid-sodium citrate buffer (pH 4.8) at a final concentration of 0.05 M. After incubation at 50 °C, 150 rpm for indicated time, the supernatants were measured for sugar concentrations by HPLC as previously described [30].

### 2.6. Statistical analysis

Statistical significance tests of differences between samples were performed by calculating *P* values with one-tailed homoscedastic *t*-test in the software Microsoft Office 2016 Excel (Microsoft, USA).

### 2.7. Bioinformatics analyses

The amino acid sequences of XYR1 homologs from *T. reesei* (NCBI protein acc. No. XP_006966092.1), *Trichoderma harzianum* (XP_024780881.1), *Podospora anserina* (XP_001906622.1), *Neurospora crassa* (XP_962611.1), *Fusarium oxysporum* f. sp. *lycopersici* (XP_018242228.1), *P. oxalicum* (EPS32714.1), *Aspergillus nidulans*
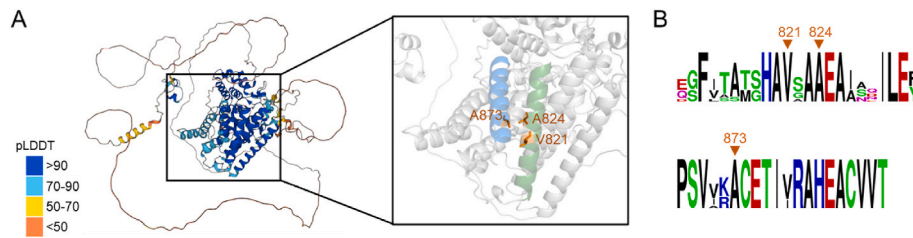
**Fig. 1.** Structural insights into the C-terminal domain of *T. reesei* XYR1. (A) The predicted structure of XYR1 in AlphaFold DB. The overall structure is colored according to per-residue confidence scores (pLDDT). Note that the amino acid sequence from 320 to 339 (VSLASPSNQFQLQLSQPIFK) was missed in the UniProt sequence (G0RLE8) used for structure prediction because of gene misannotation. In the close-up view, residues 821, 824 and 873 are shown in orange. (B) Sequence logos of the α-helix regions (811–833 and 868–887) containing V821, A824 and A873.

(Q5AVS0.2) and *A. niger* (XP_001397110.2) were aligned using Clustal Omega [31]. Sequence logos were generated based on the alignment result with the WebLogo tool [32].

Molecular dynamics (MD) simulation was performed in GROMACS 2021, and the AMBER ff99SB-ILDN force-field was used [33]. The protein atoms were put into a 9.6*9.6*9.6 nm$^3$ cubic box and solvated with water and 0.1 M NaCl. Steepest energy minimization was performed for the systems to give the maximum force below 100 kJ mol$^{-1}$ nm$^{-2}$. The temperature of the systems was slowly driven from 0 to 310 K in 2 ns to further equilibrate the systems. The MD production with three replicas was performed in the NPT ensembles with a constant temperature of 310 K. The structure model of XYR1 downloaded from AlphaFold DB [34] and deleted for amino acids 1–319 was first refined by MD simulation mentioned above for 50 ns? The final structure of this MD was used as the initial model of wide-type XYR1. The homology model of mutant XYR1$^{A873Y}$ was generated using ChimeraX by replacing A873 in wide-type initial model with a proper tyrosine rotamer [35]. A 100 ns MD was performed for both wide-type XYR1 and the mutant. Protein structures were visualized in PyMOL version 2.0 (Schrödinger, LLC).

## 3. Results and discussion

### 3.1. Location of the alanine 873 residue in the predicted structure of XYR1

The gene sequence of *T. reesei* *xyr1* was incorrectly annotated in JGI (Protein ID: 122208, http://genome.jgi.doe.gov/Trire2/Trire2.home. html) and UniProt (accession No.: G0RLE8) databases. Actually, the second intron encodes peptide VSLASPSNQFQLQLSQPIFK, and the complete sequence of *T. reesei* XYR1 contains 940 amino acid residues [13]. The protein contains a Zn$_2$Cys$_6$ DNA binding domain (92–135) and a fungal_TF_MHR domain (fungal transcription factor regulatory middle homology region, 359–843) according to the prediction by InterProScan (https://www.ebi.ac.uk/interpro/). This domain architecture is commonly observed for Gal4-like transcription factors in fungi [36]. Both domains have confidence scores higher than 50 in the result of

AlphaFold v2.0 prediction (Fig. 1A). Interestingly, the structure suggests that the amino acid residues R434 and K861 formed salt bonds with surrounding acidic residues (Fig. S1), which may provide clues for further studying the mechanisms of constitutive activation of XYR1 by their mutations [19].

The C-terminal polypeptide (346–940) of XYR1 was predicted to fold into more than ten α-helices. The two previously reported residues for engineering the activity of XYR1, V821 and A824, are located in the same α-helix (811–833), with their side chains facing that of the A873 residue in another α-helix (868–887) (Fig. 1A). Therefore, the constitutively active mutation effects of V821F and A824V might involve altered interactions between these two residues and A873. Alignment of XYR1 homologs from eight different fungal species suggested that these three residues are highly conserved, further supporting their important functions (Fig. 1B).

### 3.2. CRISPR/Cas9-based mutagenesis identified A873Y as a constitutively active mutant

CRISPR/Cas9-based genome editing is able to generate mutations at specific genomic regions without introducing selection marker gene, which is convenient for the construction and test of designed mutants. Previously, the method has been used for rapid directed mutagenesis of *xlnR* in *A. niger* [37]. Therefore, we intended to use CRISPR/Cas9 to perform random mutagenesis of the A873 codon of *xyr1* in *T. reesei*. A single guide RNA targeting the sequence upstream A873 codon was designed, and the codon GCT was replaced by degenerate sequence NNK in the donor template to introduce mutations. The PAM sequence AGG was also mutated in the donor template to avoid degradation by Cas9 (Fig. 2A). The mutated region in transformants were identified by sequencing, and four mutants (A873W, A873Y, A873R, and A873 N) were obtained after subsequent strain purification.

The parent strain QMP and mutant strains were cultivated in cellulose medium, and the culture supernatants at 120 h were compared. As shown in Fig. 2B, the extracellular protein concentration was drastically reduced when alanine 873 was mutated to tryptophan, arginine, or
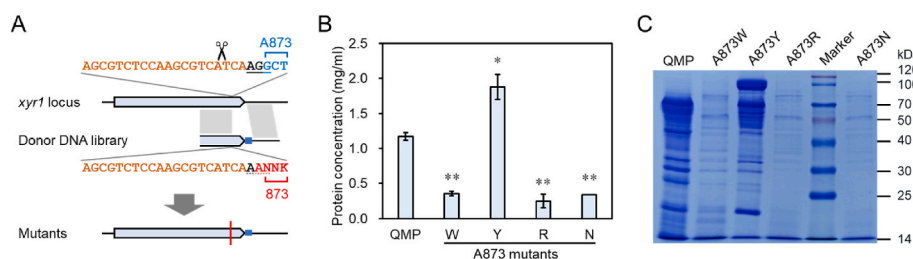


**Fig. 2.** Mutagenesis of A873 in *T. reesei* XYR1. (A) Schematic diagram of CRISPR/Cas9-aided mutagenesis. The 20-bp protospacer sequence is colored in orange. The PAM sequence is underlined. The donor templates contain homologous arms, mutated sequence (in red) and a selective PCR site (blue rectangle). (B) Extracellular protein concentrations of A873 mutation strains and parent strain QMP. The strains were cultivated in 2 % (w/v) cellulose medium for 120 h. Data represent mean ± SD from triplicate cultivations. The statistical significances of the difference between mutant strains and the parent strain are shown (*, $P < 0.05$; **, $P < 0.01$). (C) SDS-PAGE analysis of culture supernatants of equal volumes in cellulose medium at 120 h. The supernatant of parent strain QMP was used as a control.
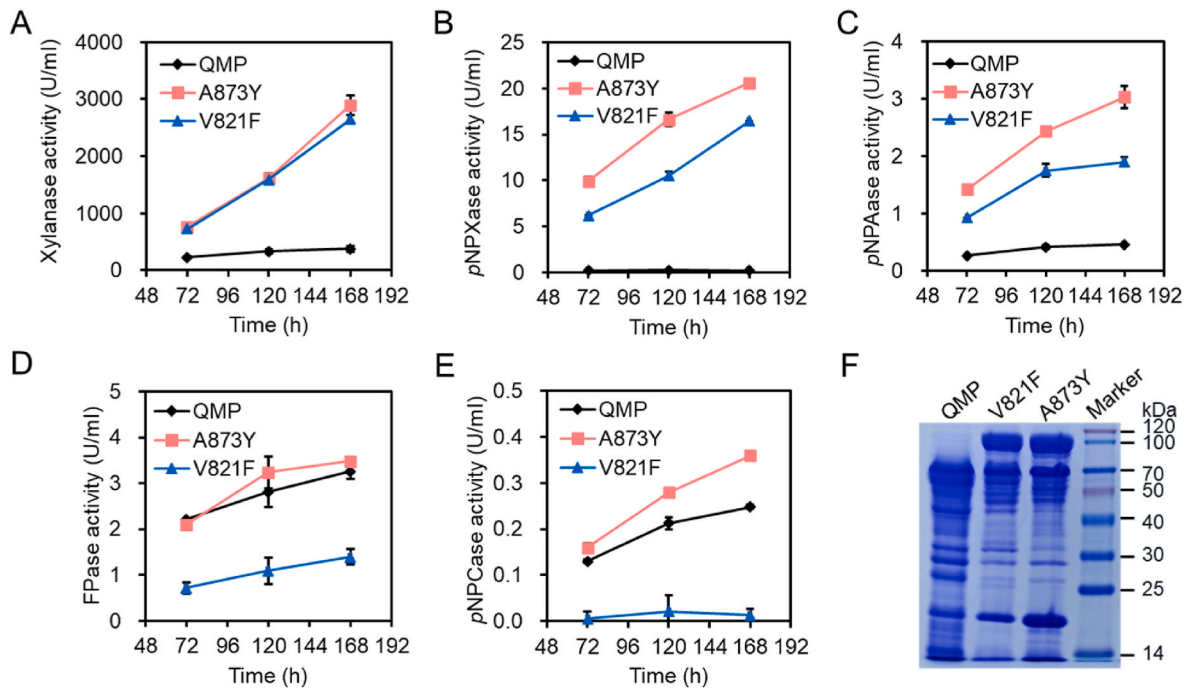
**Fig. 3.** Lignocellulolytic enzyme production by XYR1 mutated strains in 2 % (w/v) cellulose medium. (A–E) Xylanase, β-xylosidase, α-L-arabinofuranosidase, filter paper enzyme, and cellobiohydrolase activities, respectively. Data represent mean ± SD from triplicate cultivations. (F) SDS-PAGE of culture supernatants of equal volumes at 120 h.

asparagine. SDS-PAGE analysis showed that these three mutants did not produce the main cellulases and hemicellulases (Fig. 2C). In contrast, the extracellular protein concentration of A873Y mutant increased by 61 % relative to QMP, and the abundance of β-xylosidase BXL1 (97 kDa) likely increased according to SDS-PAGE analysis [17,38]. Collectively, the results suggest that alanine 873 is indeed important for the function of XYR1, and A873Y is a novel mutant of XYR1 which boosts the production of secreted proteins in *T. reesei*. The effects of mutagenesis of A873 to the other 15 residues not covered in this study are worth being studied in the future.
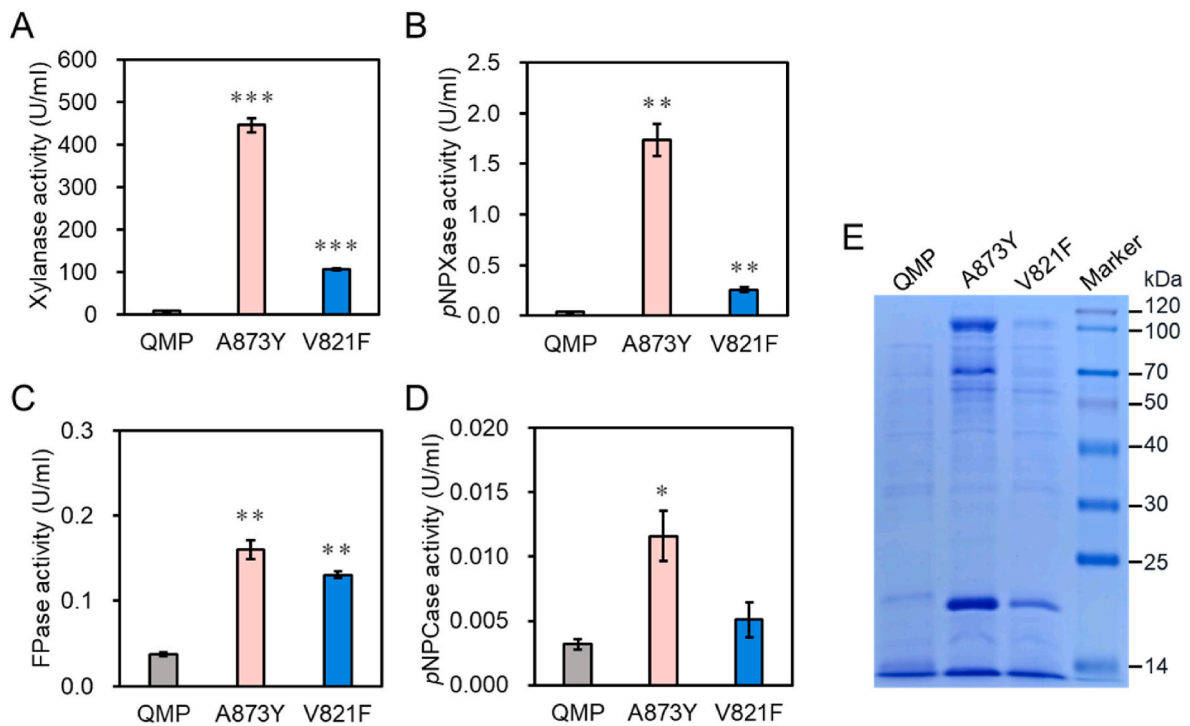


**Fig. 4.** Lignocellulolytic enzyme production by XYR1 mutated strains in 2 % (w/v) glucose medium at 120 h. (A–D) Xylanase, β-xylosidase, filter paper enzyme, and cellobiohydrolase activities, respectively. Data represent mean ± SD from triplicate cultivations. The statistical significances of the difference between mutant strains and the parent strain are shown (*, $P < 0.05$; **, $P < 0.01$; ***, $P < 0.001$). (E) SDS-PAGE of culture supernatants of equal volumes.
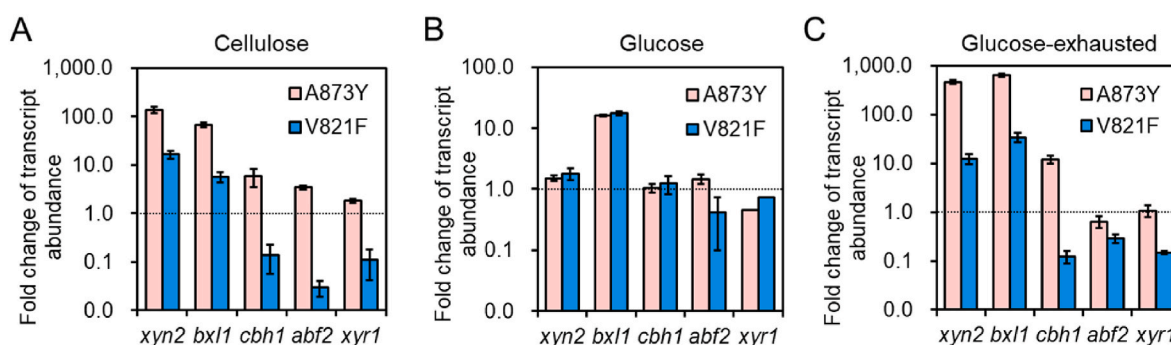
**Fig. 5.** The effects on transcript levels of lignocellulolytic enzyme encoding genes by *xyr1* mutations. Strains were precultured in 1 % (w/v) glycerol medium and thereafter transferred to media containing different carbon sources. The fold changes of transcript abundances relative to those in the parent strain are shown. Data represent mean ± SD from triplicate cultivations. (A) Transcript abundance changes in 1 % (w/v) cellulose medium at 96 h. (B, C) Transcript abundance changes in 2 % (w/v) glucose medium at 18 h and 90 h, respectively.

### 3.3. The A873Y mutation enhanced lignocellulolytic enzyme production on cellulose

The A873Y mutant strain was further compared with the parent strain QMP for the production of cellulases and hemicellulases. As a reference, the V821F mutation (GTA to TTC) was introduced to QMP, and the resulted strain was tested for enzyme production. After the cultivation in 2 % (w/v) cellulose medium for 168 h, the extracellular xylanase activity of A873Y reached 2900.0 U/ml, which was 6.7 times higher than that of QMP (Fig. 3A). At this timepoint, the β-xylosidase and α-arabinofuranosidase activities of A873Y were 20.6 U/ml and 3.0 U/ml, respectively, which were 102.1 and 5.7 times higher than those of the parent strain (Fig. 3B and C). While the overall cellulase activity measured with filter paper as substrate was less affected by the A873Y mutation, cellobiohydrolase activity of A873Y increased by 45 % compared with QMP (Fig. 3D and E).

The above results indicate that the A873Y mutation significantly elevated the production of hemicellulases associated with xylan degradation in cellulose medium. In agree with the results of enzyme activity measurement, the bands corresponding to BXL1 and XYN1/XYN2 (21 kDa) remarkably increased in A873Y (Fig. 3F). Notably, the β-xylosidase and α-L-arabinofuranosidase activities of A873Y were higher those of the V821F mutant. The decreases of cellulolytic activities in the V821F mutant were surprising. It should be noted that the *xyr1* mutants were expressed under the control of the native promoter in this study. When the *xyr1*$^{V821F}$ mutant was expressed using a constitutive promoter (Ppdc1), the production of extracellular cellulases was increased in cellulose medium, despite that their proportions in the secretome declined [16].

### 3.4. Inducer-independent expression of lignocellulolytic enzymes in the A873Y mutant

Glucose is a typical repressing carbon source for the expression of biomass-degrading enzymes in microorganisms. Considering that the expression of XYR1$^{V821F}$ and XYR1$^{A824V}$ both resulted in lignocellulolytic enzyme production on glucose (i.e. the "glucose blind" phenotype) [13,16], the enzyme-producing ability of A873Y mutant was also studied in 2 % (w/v) glucose medium. After 120 h of cultivation, the extracellular xylanase and β-xylosidase activities of the A873Y strain reached 445.4 U/ml and 1.7 U/ml, respectively, whereas the above enzyme activities were almost undetectable in the culture supernatant of the parent strain QMP (Fig. 4A and B). Meanwhile, A873Y showed significantly enhanced production of filter paper enzyme and cellobiohydrolase activities compared with QMP (Fig. 4C and D). SDS-PAGE analysis of culture supernatants showed that there were few extracellular proteins in the parent strain, whereas protein bands corresponding to xylanases, β-xylosidase and cellulases (50–70 kDa) were observed for

A873Y (Fig. 4E). The above results indicated that the A873Y mutation of XYR1 has the ability to activate xylanase and cellulase production under inducer-free condition. Similar with the results in cellulose medium, the A873Y mutation improved lignocellulolytic enzyme production to higher levels than those by the V821F mutation.

### 3.5. Changes in the transcript abundances of lignocellulolytic enzyme genes in the A873Y mutant

To further investigate the regulatory mechanism of the XYR1$^{A873Y}$ mutant, we examined the transcript levels of four genes encoding representative lignocellulolytic enzymes using quantitative PCR. These include *xyn2*, *bxl1*, *cbh1*, and *abf2*, which encode xylanase II, β-xylosidase I, cellobiohydrolase I and α-L-arabinofuranosidase II, respectively. As shown in Fig. 5A, transcript levels of all four genes in cellulose medium increased in A873Y relative to the parent, suggesting that the enhanced enzyme production observed in this mutant is due to the higher mRNA levels of corresponding genes. The results also confirmed that XYR1$^{A873Y}$ has a stronger ability to improve the expression of lignocellulolytic enzymes than XYR1$^{V821F}$.

The mRNA levels of the selected genes were studied at two timepoints for the cultures on glucose. After 18 h of cultivation with about 6 g/L glucose retained in the medium, the A873Y and V821F mutants had similar transcript levels for all tested genes. Only the *bxl1* transcript showed approximately 16-fold higher abundance relative to the parent strain, while the levels of the other three genes were essentially unchanged (Fig. 5B). However, at 90 h when glucose had been exhausted, the transcript levels of *xyn2*, *bxl1* and *cbh1* increased by 461-, 636-, and 11-fold, respectively, in A873Y over the parent strain (Fig. 5C). Increased transcript levels of *xyn2* and *bxl1* were also detected for the V821F mutant in glucose medium at 90 h. Compared with the lignocellulolytic enzyme-encoding genes, the transcript level of *xyr1* itself was less changed in the A873Y mutant under all three conditions. However, the *xyr1* level was decreased by about 90 % in the V821F mutant under cellulose and glucose-exhausted conditions. The transcription of *xyr1* was reported to be negatively auto-regulated via a XYR1-binding element in its promoter [39]. Whether this negative regulation is strengthened in the V821F mutant remains unknown.

The above results suggested that the mechanims for the enhanced transcriptional activation by XYR1$^{A873Y}$ is complicated. Firstly, the improvement of lignocellulolytic enzyme production is biased towards xylanolytic enzymes. This phenomenon was also observed in previous studies on V821F and A824V mutants [16,17] as well as some domain-reshuffled mutants of XYR1 [40,41]. The sequence or domain modifications of XYR1 might change its DNA-binding affinities or interactions with other regulatory proteins. Secondly, the effects of XYR1$^{A873Y}$ on lignocellulolytic enzyme expression are condition-dependent. Particularly, overall cellulase activity was only
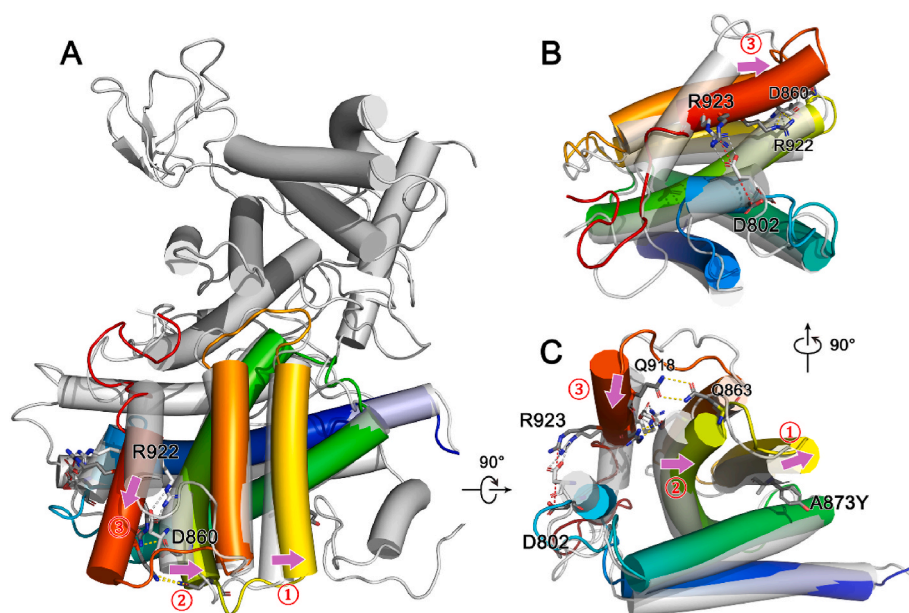
**Fig. 6.** Comparison of the structures of XYR1 wild type and A873Y mutant after MD. The wild-type structure is depicted in gray, while the mutant's 765–940 domain is depicted in a rainbow spectrum. The α-helix offset directions are denoted by violet arrows, and labeled with numbers in red circles for reference. Key amino acid residues are presented in stick models. Interactions in the wild-type structure are illustrated with gray dashed lines, while those in the A873Y mutant are highlighted with yellow dashed lines. The disruption of the D802-R923 salt bond is indicated by a red dashed line. (A–C) Three different perspectives of the conformational changes.

increased in the glucose medium (glucose-exhausted condition, more specifically), while no "hyper-induction" was observed in cellulose medium. Finally, previous studies on the point mutants of XYR1 usually use constitutive promoters (e.g. P*tef1*, P*pdc1* and P*act1*) to control their expression. The effect of XYR1$^{A873Y}$ overexpression on enzyme-producing levels is worth being investigated in the future.
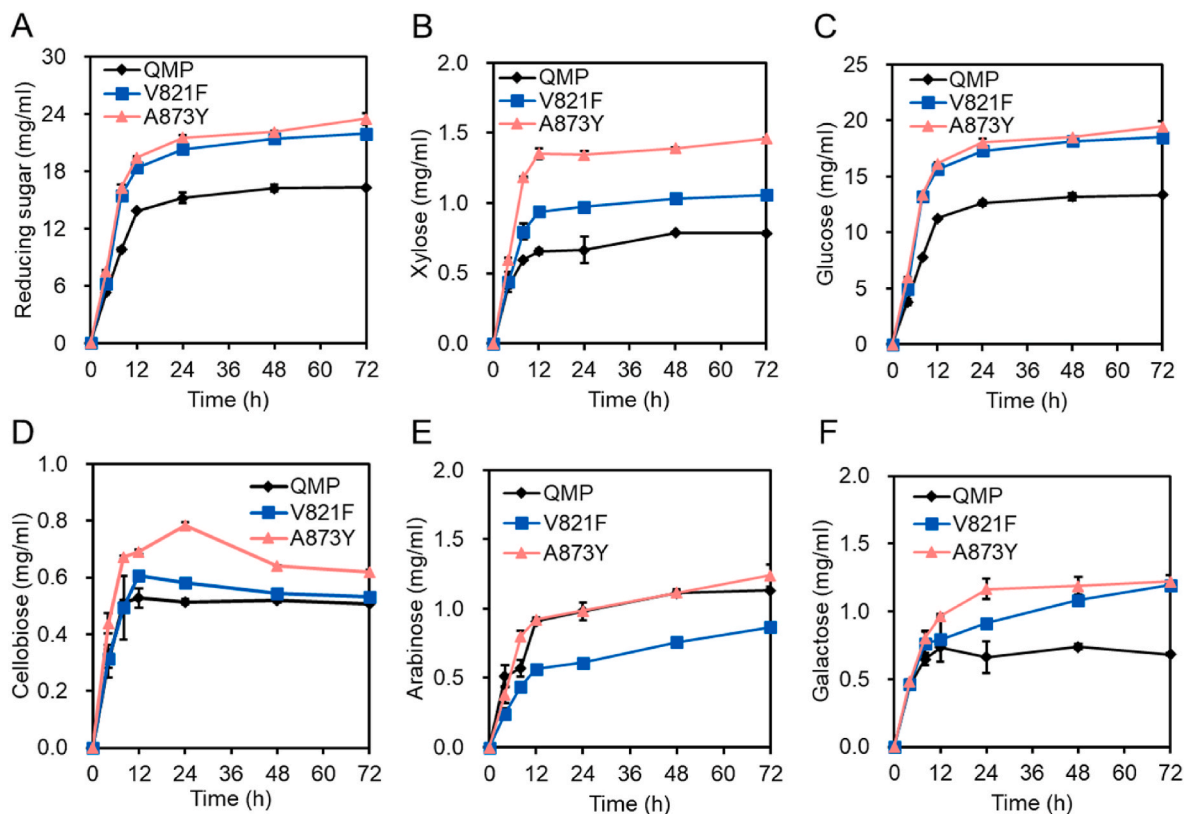


**Fig. 7.** Releases of sugars from corn fiber by crude enzymes of *T. reesei* strains. The concentrations of total reducing sugar (A), xylose (B), glucose (C), cellobiose (D), arabinose (E) and galactose (F) are shown. Data represent mean ± SD from triplicate cultivations.
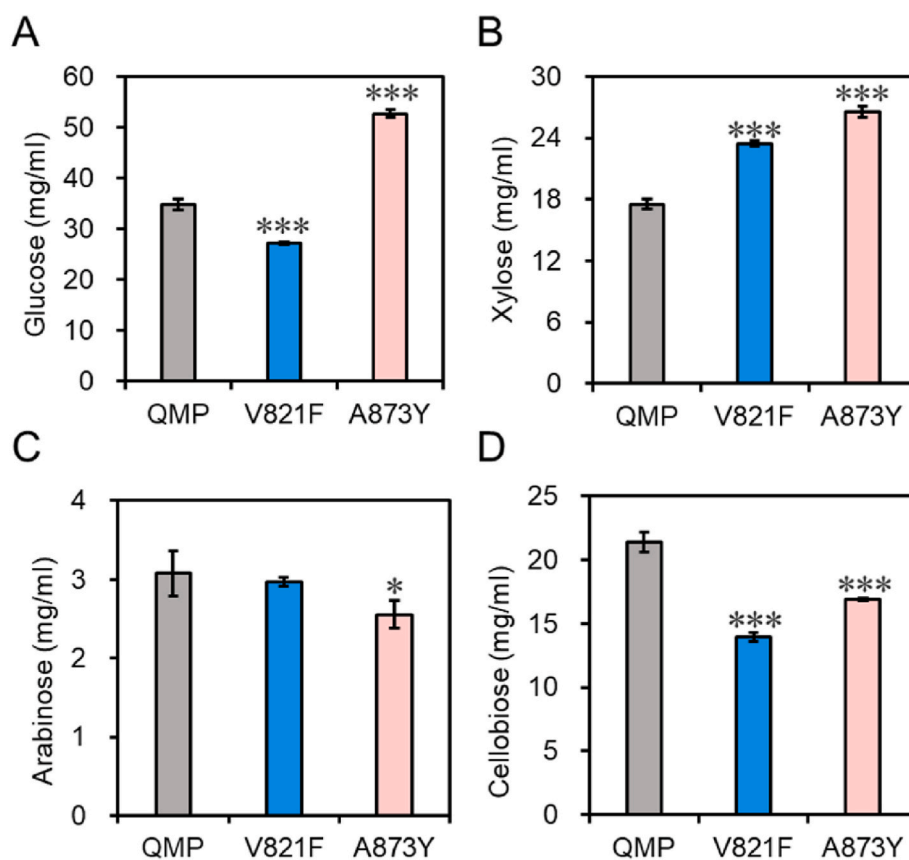
**Fig. 8.** Releases of sugars from alkali pretreated corn stover by crude enzymes of *T. reesei* strains. The concentrations of glucose (A), xylose (B), arabinose (C) and cellobiose (D) at 72 h are shown. Data represent mean ± SD from triplicate cultivations. The statistical significances of the difference between mutant strains and the parent strain QMP are shown (***, $P < 0.001$).

### 3.6. Possible conformational changes of XYR1 caused by the A873Y mutation

So far, the constitutive activation of XYR1 by point mutations lacks credible explanations. Generally, the mutations are supposed to affect the structural conformation of XYR1, turning it to the activated configuration [13,19]. Indeed, an *in vitro* study revealed that XYR1[A824V] had reduced DNA-binding affinity and loss of α-helix structures compared with the wild type [42]. To investigate the possible changes of XYR1 structure caused by the A873Y mutation, the wild-type and mutated structures were subjected to MD simulations. The results highlighted substantial conformational distinctions between the two models (Fig. 6). Notably, the A873Y mutation resulted in a larger side chain, causing conflicts and shifting the α-helix 868–884 (Fig. 6 arrow 1). This conformational change propagated a shift of α-helix 841–862 through loop 863–867 (arrow 2), leading to the displacement of D860. Consequently, the salt bond between D860-R922 prompted α-helix 918–928 to rotate (arrow 3). Simultaneously, Q863 and Q918 established a new electrostatic interaction, further stabilizing the new conformation of the last α-helix. As a result, the salt bond between D802 and R923 was disrupted. Upon inspecting the structure, we speculate that both V821F and A824V mutations would induce a shift of α-helix 868–884 along arrow 1 due to the larger side chains, leading to a conformational change similar to A873Y.

The 767–860 region of XYR1 was previously found to be able to recruit transcription machinery by interacting with the KIX domain of Mediator subunit Gal11 [12]. Roughly the same region (771–865) was reported to interact with another cellulase master regulator ACE3 [43]. In addition, the C-terminal residues 861–940 mediate the homodimerization of XYR1, which is essential for cellulase expression [43]. The conformational changes caused by A873Y mutation (Fig. 6) may affect the above protein-protein interactions and results in constitutive cellulase expression. In addition, the possible effects of the mutation in the stability, cellular localization and other characteristics (e.g. DNA binding ability) of XYR1 cannot be excluded. Although the deletion of 701–940 region does not affect the production of xylanase [43], the significantly activated xylanase expression in A873Y and V821F mutants indicates that this region may be involved in the modulation of XYR1's activity in response to upstream signals.

### 3.7. Crude enzymes produced by the A873Y mutant showed enhanced performance in lignocellulose degradation

Considering that the A873Y mutant produced enzyme cocktails with the enrichment of xylanolytic activities (Fig. 3), the crude enzymes were tested for their hydrolytic efficiency on corn fiber, a xylan-rich byproduct of corn wet-milling. As shown in Fig. 7A, crude enzymes of A873Y mutant produced 44 % higher total reducing sugars than those of the parent strain QMP at 72 h, when equal amounts of proteins were loaded. Further HPLC analysis of the hydrolysates showed an 86 % increase in xylose production by A873Y mutant compared with QMP, and the increase was greater than the V821F mutant (Fig. 7B). After 72 h of reaction, the glucose concentration in the hydrolysate of the A873Y mutant reached 19.4 mg/ml, 46 % higher than that of QMP (Fig. 7C). Cellobiose was accumulated during the first 24 h and declined slowly afterwards, suggesting that the level of β-glucosidase in the enzyme system needs to be improved (Fig. 7D). Surprisingly, the concentrations of arabinose in the hydrolysates of QMP and A873Y were essentially the same, while that in the hydrolysate of V821F was 23 % lower than QMP (Fig. 7E). The different results between arabinose release from corn fiber

and *p*NPAase activity measurement (Fig. 3C) highlighted that synthetic substrate analogs may not be suitable for evaluating the activity of lignocellulolytic enzymes [44]. Finally, crude enzymes of A873Y produced 79 % more galactose than those of QMP, and a faster release of galactose was observed for A873Y enzymes compared with those of V821F (Fig. 7F).

The hydrolysis efficiencies of the crude enzymes were also compared on alkali pretreated corn stover. As shown in Fig. 8A and **B**, after 72 h of saccharification, the concentrations of glucose and xylose in the hydrolysate of A873Y were 51 % and 52 % higher than that of QMP, respectively. The concentrations of glucose and xylose were also higher than those using the enzymes produced by V821F mutant. Reducing sugars from corn stover by A873Y was higher than V821F at the same time. The concentration of arabinose as a minor product was decreased by 17 % in the hydrolysate of A873Y (Fig. 8C). The concentration of cellobiose in the hydrolysate of A873Y mutant was significantly reduced relative to that of QMP, but the data suggest that β-glucosidase activity in the mutant strain still needs to be improved to achieve higher glucose production (Fig. 8D).

## 4. Conclusions

In this study, a novel constitutively active mutant XYR1$^{A873Y}$ was identified in *T. reesei* based on the predicted structure of XYR1. The strain carrying this mutant showed significantly enhanced production of xylanolytic enzymes in cellulose medium, and expression of lignocellulolytic enzymes was activated under the inducer-free conditions. The crude enzymes produced by the mutant strain showed a better performance in the saccharification of corn fiber and pretreated corn stover compared with those of parent strain of the same protein loading. These findings provide an efficient strategy for improving the production level and performance of lignocellulolytic enzyme system in *T. reesei*.

## Data availability statement

The data used to support the findings of this study are available from the corresponding authors upon request.

## CRediT authorship contribution statement

**Qinqin Zhao:** Investigation, Data curation, Formal analysis, Writing – original draft. **Zezheng Yang:** Investigation, Writing – original draft. **Ziyang Xiao:** Investigation. **Zheng Zhang:** Investigation. **Jing Xing:** Investigation. **Huiqi Liang:** Investigation. **Liwei Gao:** Methodology, Data curation, Funding acquisition. **Jian Zhao:** Data curation, Resources. **Yinbo Qu:** Data curation, Resources. **Guodong Liu:** Conceptualization, Data curation, Funding acquisition, Supervision, Writing – review & editing.

## Declaration of competing interest

The authors declare the following financial interests/personal relationships which may be considered as potential competing interests: A patent "A mutant of regulatory protein for lignocellulolytic enzyme synthesis in fungi and its applications" based on the research in this study has been filed.

## Acknowledgements

## Appendix A. Supplementary data

Supplementary data to this article can be found online at https://doi.org/10.1016/j.synbio.2023.11.005.

## References

[1] Madhavan A, Arun KB, Sindhu R, Nair BG, Pandey A, Awasthi MK, et al. Design and genome engineering of microbial cell factories for efficient conversion of lignocellulose to fuel. Bioresour Technol 2023;370:128555.

[2] Huberman LB, Liu J, Qin L, Glass NL. Regulation of the lignocellulolytic response in filamentous fungi. Fungal Biol Rev 2016;30:101–11.

[3] Sukumaran RK, Christopher M, Kooloth-Valappil P, Sreeja-Raju A, Mathew RM, Sankar M, et al. Addressing challenges in production of cellulases for biomass hydrolysis: targeted interventions into the genetics of cellulase producing fungi. Bioresour Technol 2021;329:124746.

[4] Xue Y, Han J, Li Y, Liu J, Gan L, Long M. Promoting cellulase and hemicellulase production from *Trichoderma orientalis* EU7-22 by overexpression of transcription factors Xyr1 and Ace3. Bioresour Technol 2020;296:122355.

[5] Gao L, Xu Y, Song X, Li S, Xia C, Xu J, et al. Deletion of the middle region of the transcription factor ClrB in *Penicillium oxalicum* enables cellulase production in the presence of glucose. J Biol Chem 2019;294:18685–97.

[6] Wang Y, Ren M, Wang Y, Wang L, Liu H, Shi M, et al. Constitutive overexpression of cellobiohydrolase 2 in *Trichoderma reesei* reveals its ability to initiate cellulose degradation. Eng Microbiol 2023;3:100059.

[7] Bischof RH, Ramoni J, Seiboth B. Cellulases and beyond: the first 70 years of the enzyme producer *Trichoderma reesei*. Microb Cell Factories 2016;15:106.

[8] Zhang X, Li Y, Zhao X, Bai F. Constitutive cellulase production from glucose using the recombinant *Trichoderma reesei* strain overexpressing an artificial transcription activator. Bioresour Technol 2017;223:317–22.

[9] Stricker AR, Grosstessner-Hain K, Wurleitner E, Mach RL. Xyr1 (xylanase regulator 1) regulates both the hydrolytic enzyme system and D-xylose metabolism in *Hypocrea jecorina*. Eukaryot Cell 2006;5:2128–37.

[10] Dos Santos Castro L, de Paula RG, Antonieto AC, Persinoti GF, Silva-Rocha R, Silva RN. Understanding the role of the master regulator XYR1 in *Trichoderma reesei* by global transcriptional analysis. Front Microbiol 2016;7:175.

[11] Lichius A, Seidl-Seiboth V, Seiboth B, Kubicek CP. Nucleo-cytoplasmic shuttling dynamics of the transcriptional regulators XYR1 and CRE1 under conditions of cellulase and xylanase gene expression in *Trichoderma reesei*. Mol Microbiol 2014;94:1162–78.

[12] Zheng F, Cao Y, Yang R, Wang L, Lv X, Zhang W, et al. *Trichoderma reesei* XYR1 activates cellulase gene expression via interaction with the Mediator subunit TrGAL11 to recruit RNA polymerase II. PLoS Genet 2020;16:e1008979.

[13] Derntl C, Gudynaite-Savitch L, Calixte S, White T, Mach RL, Mach-Aigner AR. Mutation of the xylanase regulator 1 causes a glucose blind hydrolase expressing phenotype in industrially used *Trichoderma* strains. Biotechnol Biofuels 2013;6:62.

[14] Xia C, Gao L, Li Z, Liu G, Song X. Functional analysis of the transcriptional activator XlnR of *Penicillium oxalicum*. J Appl Microbiol 2022;132:1112–20.

[15] Hasper AA, Trindade LM, van der Veen D, van Ooyen AJ, de Graaff LH. Functional analysis of the transcriptional activator XlnR from *Aspergillus niger*. Microbiology 2004;150:1367–75.

[16] Ellilä S, Fonseca L, Uchima C, Cota J, Goldman GH, Saloheimo M, et al. Development of a low-cost cellulase production process using *Trichoderma reesei* for Brazilian biorefineries. Biotechnol Biofuels 2017;10:30.

[17] Arai T, Ichinose S, Shibata N, Kakeshita H, Kodama H, Igarashi K, et al. Inducer-free cellulase production system based on the constitutive expression of mutated XYR1 and ACE3 in the industrial fungus *Trichoderma reesei*. Sci Rep 2022;12:19445.

[18] Arai T, Ichinose S. Mutant filamentous fungus, and method for producing protein using same. 2021. Patent WO/2021/100631.

[19] Lv D, Zhang W, Meng X, Liu W. Single mutation in transcriptional activator Xyr1 enhances cellulase and xylanase production in *Trichoderma reesei* on glucose. J Agric Food Chem 2023;71:11993–2003.

[20] Jumper J, Evans R, Pritzel A, Green T, Figurnov M, Ronneberger O, et al. Highly accurate protein structure prediction with AlphaFold. Nature 2021;596:583–9.

[21] Li Y, Reed M, Wright HT, Cropp TA, Williams GJ. Development of genetically encoded biosensors for reporting the methyltransferase-dependent biosynthesis of semisynthetic macrolide antibiotics. ACS Synth Biol 2021;10:2520–31.

[22] Li J, Liu R, Chen Y, Liu S, Chen C, Liu T, et al. Computer-aided rational engineering of signal sensitivity of quorum sensing protein LuxR in a whole-cell biosensor. Front Mol Biosci 2021;8:729350.

[23] Findlay GM, Boyle EA, Hause RJ, Klein JC, Shendure J. Saturation editing of genomic regions by multiplex homology-directed repair. Nature 2014;513:120–3.

[24] Wei J, Li Y. CRISPR-based gene editing technology and its application in microbial engineering. Eng Microbiol 2023;3:100101.

[25] Wang Q, Zhao Q, Liu Q, He X, Zhong Y, Qin Y, et al. CRISPR/Cas9-mediated genome editing in *Penicillium oxalicum* and *Trichoderma reesei* using 5S rRNA promoter-driven guide RNAs. Biotechnol Lett 2021;43:495–502.

[26] Gao L, Li Z, Xia C, Qu Y, Liu M, Yang P, et al. Combining manipulation of transcription factors and overexpression of the target genes to enhance lignocellulolytic enzyme production in *Penicillium oxalicum*. Biotechnol Biofuels 2017;10:100.

[27] Jiang S, Wang Y, Liu Q, Zhao Q, Gao L, Song X, et al. Genetic engineering and raising temperature enhance recombinant protein production with the *cdna1* promoter in *Trichoderma reesei*. Bioresour Bioprocess 2022;9:113.

[28] Livak KJ, Schmittgen TD. Analysis of relative gene expression data using real-time quantitative PCR and the $2_T^{-\Delta\Delta C}$ Method. Methods 2001;25:402–8.

[29] Steiger MG, Mach RL, Mach-Aigner AR. An accurate normalization strategy for RT-qPCR in *Hypocrea jecorina* (*Trichoderma reesei*). J Biotechnol 2010;145:30–7.

[30] Gao L, He X, Guo Y, Wu Z, Zhao J, Liu G, et al. Combinatorial engineering of transcriptional activators in *Penicillium oxalicum* for improved production of corn-fiber-degrading enzymes. J Agric Food Chem 2021;69:2539–48.

[31] Madeira F, Pearce M, Tivey ARN, Basutkar P, Lee J, Edbali O, et al. Search and sequence analysis tools services from EMBL-EBI in 2022. Nucleic Acids Res 2022; 50:W276–9.

[32] Crooks GE, Hon G, Chandonia JM, Brenner SE. WebLogo: a sequence logo generator. Genome Res 2004;14:1188–90.

[33] Lindorff-Larsen K, Piana S, Palmo K, Maragakis P, Klepeis JL, Dror RO, et al. Improved side-chain torsion potentials for the Amber ff99SB protein force field. Proteins 2010;78:1950–8.

[34] Varadi M, Anyango S, Deshpande M, Nair S, Natassia C, Yordanova G, et al. AlphaFold Protein Structure Database: massively expanding the structural coverage of protein-sequence space with high-accuracy models. Nucleic Acids Res 2022;50:D439–44.

[35] Pettersen EF, Goddard TD, Huang CC, Meng EC, Couch GS, Croll TI, et al. UCSF ChimeraX: structure visualization for researchers, educators, and developers. Protein Sci 2021;30:70–82.

[36] MacPherson S, Larochelle M, Turcotte B. A fungal family of transcriptional regulators: the zinc cluster proteins. Microbiol Mol Biol Rev 2006;70:583–604.

[37] Kun RS, Meng J, Salazar-Cerezo S, Makela MR, de Vries RP, Garrigues S. CRISPR/Cas9 facilitates rapid generation of constitutive forms of transcription factors in *Aspergillus niger* through specific on-site genomic mutations resulting in increased saccharification of plant biomass. Enzym Microb Technol 2020;136:109508.

[38] Herpoel-Gimbert I, Margeot A, Dolla A, Jan G, Molle D, Lignon S, et al. Comparative secretome analyses of two *Trichoderma reesei* RUT-C30 and CL847 hypersecretory strains. Biotechnol Biofuels 2008;1:18.

[39] Till P, Derntl C, Kiesenhofer DP, Mach RL, Yaver D, Mach-Aigner AR. Regulation of gene expression by the action of a fungal lncRNA on a transactivator. RNA Biol 2020;17:47–61.

[40] Derntl C, Mach RL, Mach-Aigner AR. Fusion transcription factors for strong, constitutive expression of cellulases and xylanases in *Trichoderma reesei*. Biotechnol Biofuels 2019;12:231.

[41] Lv D, Zhang W, Meng X, Liu W. A novel fusion transcription factor drives high cellulase and xylanase production on glucose in *Trichoderma reesei*. Bioresour Technol 2023;370:128520.

[42] Mello-de-Sousa TM, Gorsche R, Jovanovic B, Mach RL, Mach-Aigner AR. In vitro characterization of a nuclear receptor-like domain of the Xylanase Regulator 1 from *Trichoderma reesei*. J Fungi (Basel) 2022;8:1254.

[43] Zhang J, Chen Y, Wu C, Liu P, Wang W, Wei D. The transcription factor ACE3 controls cellulase activities and lactose metabolism via two additional regulators in the fungus *Trichoderma reesei*. J Biol Chem 2019;294:18435–50.

[44] Liu G, Qu Y. Integrated engineering of enzymes and microorganisms for improving the efficiency of industrial lignocellulose deconstruction. Eng Microbiol 2021;1: 100005.